AFRL-SR-BL-TR-98-

REPORT DOCUMENTATION PAGE

0575

1. AGENCY USE ONLY (Leave blank)	2. REPORT DATE	3. REPORT TYPE AND DATES COVERED
		Final 01 Apr 95 to 31 Mar 98

4. TITLE AND SUBTITLE
Diagnostics and storage of turbulence distorted wavefronts by using spectral hole buring materials

5. FUNDING NUMBERS
61102F
2305/DS

6. AUTHOR(S)
Dr Kachru

7. PERFORMING ORGANIZATION NAME(S) AND ADDRESS(ES)
SRI International
333 Ravenswood Avenue
Menlo Park CA 94025-3493

8. PERFORMING ORGANIZATION REPORT NUMBER

9. SPONSORING/MONITORING AGENCY NAME(S) AND ADDRESS(ES)
AFOSR/NE
110 Ducan Ave RmB115
Bolling AFB DC 20332-8050

10. SPONSORING/MONITORING AGENCY REPORT NUMBER
F49620-95-C-0029

11. SUPPLEMENTARY NOTES

12a. DISTRIBUTION/AVAILABILITY STATEMENT
APPROVAL FOR PUBLIC RELEASED: DISTRIBUTION UNLIMITED

12b. DISTRIBUTION CODE

13. ABSTRACT *(Maximum 200 words)*

SRI International has completed a program of research on an innovative time-differential phase sensor suitable for detecting the fast changing structure within airborne turbulence. This innovation is based on an orginal incorporation of time-domain-stimulated photon echo into a phase-conjugate-mirror of an optical novelty filter setup. The unique advantage of this photon echo novelty filter is that its fast response time is completely programmable through external excitation timing. Therefore, it has an outstnading potential for tracking fast changing phase distortions in real time.

14. SUBJECT TERMS			15. NUMBER OF PAGES
			16. PRICE CODE
17. SECURITY CLASSIFICATION OF REPORT	18. SECURITY CLASSIFICATION OF THIS PAGE	19. SECURITY CLASSIFICATION OF ABSTRACT	20. LIMITATION OF ABSTRACT
UNCLASSIFED	UNCLASSIFIED	UNCLASSIFIED	UL

NSN 7540-01-280-5500

Standard Form 298 (Rev. 2-89)
Prescribed by ANSI Std. 239-18

SRI International

Final Report • May 1998

DIAGNOSTICS AND STORAGE OF TURBULENCE DISTORTED WAVEFRONTS BY USING SPECTRAL HOLE-BURNING MATERIALS

Prepared by:

Ravinder Kachru, Senior Physicist
Yiping Zhang, Postdoctoral Associate
Molecular Physics Laboratory

Contract No. F49620-95-C-0029
MP 98-006

Prepared for:

Air Force Office of Scientific Research
110 Duncan Avenue, Suite B115
Bolling AFB, DC 20332-0001

Attn: Dr. Alan Craig

Approved by:

David R. Crosley, Director
Molecular Physics Laboratory

333 Ravenswood Avenue • Menlo Park, CA 94025-3493 • (650) 859-2000

ABSTRACT

SRI International has completed a program of research on an innovative time-differential phase sensor suitable for detecting the fast changing structure within airborne turbulence. This innovation is based on an original incorporation of time-domain-stimulated photon echo into a phase-conjugate-mirror of an optical novelty filter setup. The unique advantage of this photon echo novelty filter is that its fast response time is completely programmable through external excitation timing. Therefore, it has an outstanding potential for tracking fast changing phase distortions in real time.

Using Eu and Pr doped yttrium silicate crystal as the hole-burning materials for the stimulated photon echo, we demonstrated the concept and basic performance of the photon echo novelty filter. The sensitivity of the filter to a sudden change of optical path length is measured to be better than 0.05 wavelength (~0.6 μm). The fast temporal tracking ability of the filter is proved by its accurate measurement of phase modulation events from a nanosecond through microsecond time scale. The filter's holographic memory and time-differential processing of nonuniform phase-only distortion is proved. Our results show that the photon echo novelty filter is well worth further investigation and development into a powerful sensor of the temporal and spatial structures of airborne turbulence.

CONTENTS

INTRODUCTION

Airborne turbulence has been a long-standing problem in aero-optics [1]. Optical imaging and the laser projection wavefront from a flying airplane platform are strongly distorted by the surrounding turbulent air layer that the light traverses. This problem becomes much more severe for rear looking directions [2] and is aggravated by the turbulence's fast change and short coherence time on microsecond time scale [3]. The coherence time is three orders of magnitude shorter than the response time of current adaptive optics [4]. A need for a correspondingly fast phase sensor and compensator is thus evident. Because little is known about the temporal and spatial structures inside airborne turbulence, a reasonable approach to the problem is to study the turbulence using a fast time-differential phase sensor that can temporally resolve the fast change.

An optical novelty filter is a suitable tool for resolving the fast-changing feature in an optical input [5]. Conventional optical novelty filters are based mainly on photorefractive crystals, which take milliseconds to react to a constantly changing input [6]. Clearly, a new novelty filter is needed to react to the fast and constantly changing input through airborne turbulence.

This report describes a new optical novelty filter based on spectral hole-burning crystals through time-domain stimulated photon echo. This new filter is unique in its programmable response time, which can be changed from nanoseconds to microseconds.

Stimulated photon echo technologies have been developed by SRI International for many years [7-9]. Our good understanding of the basic physics and optical memory application of stimulated photon echo in spectral hole-burning crystals encouraged us to construct a phase-only optical memory and a phase-conjugate-mirror installed in the new novelty filter.

During the past two years, we demonstrated the concept and basic performances of the photon echo novelty filter to detect fast phase changes. We showed that the filter is fully capable of real time resolving a fast phase change from a nanosecond to microsecond time scale [10,11]. The filter was found to be more suitable for detecting a fast phase change within 20 μs than for slower ones because of its intrinsic high-pass feature. We suppressed the background of the filter to an equivalent phase change below 0.05 wavelength (~0.6 μm). The accuracy and resolution of the filter were found to be 0.02 wavelength. The filter's holographic phase-only memory is proved by the phase-conjugate recalling of a random phase map [11]. These results provide the basis for future development of the filter into a real time tracking sensor of fast phase change through airborne turbulence.

BACKGROUND

AIRBORNE TURBULENCE

For an airplane flying at the speed of sound, the air surrounding the plane is dragged by the plane to move forward at a similar speed. However, a boundary layer of air adheres to the front of the plane's body. The flow inside this boundary layer is nearly laminar and does not distort a light wave going through it very much [2], partly because the air in the boundary layer has a very small speed transverse to a forward going light wave. The wind speed longitudinal to the optical wave produces no wavefront distortion. Therefore, the Strehl ratio is quite high in the forward direction (azimuthal angle close to 0°).

For a light wave going at an azimuthal angle substantially larger than zero but less than 90°, the air in the boundary layer has a large transverse speed across its wavefront. Consequently, the wavefront is distorted and the Strehl ratio is smaller. However, because the flow in the boundary layer is laminar, the air density and the index of refraction do not fluctuate very much. Therefore, the wavefront is not severely distorted at the front of the plane and the Strehl ratio is tolerable.

The picture changes completely at the back of the airplane (see Figure 1). The boundary layer begins to be separated from the body of the plane at an azimuthal angle of 90°, and this separation is more prominent at larger azimuthal angles [2]. In the latter region, the boundary layer becomes a completely separated flow. This flow still moving at a high speed with the plane, is surrounded by the ambient air, which is only drifting slowly. The large velocity difference at the interface between the separated flow and the ambient air creates a shear layer that is fully turbulent [2], and the strength of turbulence is very strong in that region. The strong fluctuations of air density cause strong fluctuations of the index of refraction.

To make things worse, the shear layer is projected over a long distance behind the plane. An optical beam propagating at large azimuthal angle inevitably travels a long path length through this shear layer, which accumulates into great wavefront distortions. For the same path length, the corresponding wavefront distortion is less serious for longer optical wavelength. However, shorter wavelength is favored in applications requiring tighter diffraction limited focus. To show how severe the problem is, it has been reported that the phase distortion at the back of an airplane turret can approach nearly two wavelengths (~0.7 μm) [2].

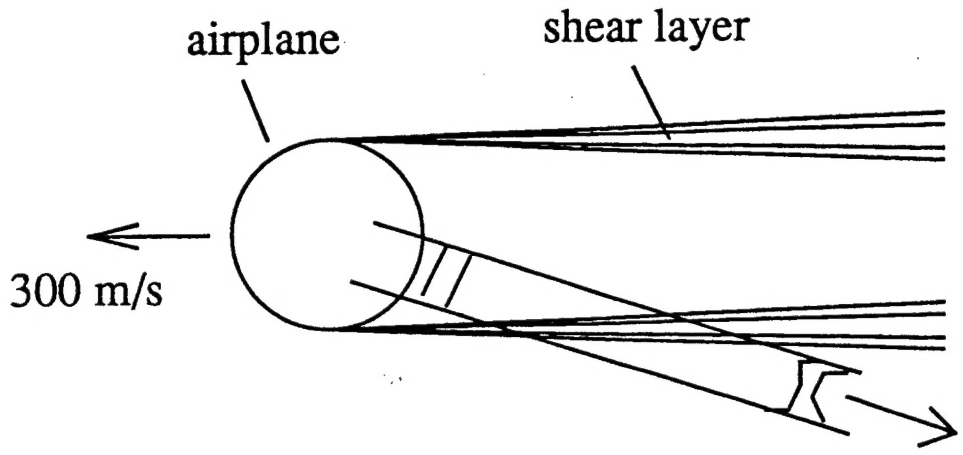

Figure 1.

The other harsh character of airborne turbulence is its fast change and short coherence time. The phase distortion is reported to rise to 80% of its full-scale value within approximately 200 μs. In other words, the turbulent phase change is coherently trackable only within about 200 μs. To correct this phase distortion, an adaptive system needs to measure the phase and initiate a compensation within that coherence time. This time is much shorter than the response time of Shack-Hartmann sensor and deformable mirrors within the current adaptive optics technologies [4].

Such high bandwidth is also predicted in theory by the Greenwood frequency [12], which is defined as the bandwidth required to fully compensate for wavefront distortion. When the transverse wind velocity is constant along the optical path, the Greenwood frequency can be written as

$$f_G = 0.426\ v/r_0$$

where v is the wind velocity and r_0 is the Fried parameter [12] for the turbulence; v is approximately 200 m/s for the wind around an airplane flying at a Mach number of one. r_0 is defined as

$$r_0 = 0.185(\lambda^2/C_n^2\Delta z)^{3/5}$$

where λ is the optical wavelength, C_n^2 is the refractive index structure constant, which tells the strength of fluctuations of the index of refraction, and Δz is the length of the optical path, or the thickness of the turbulence layer.

C_n^2 is defined for an isotropic turbulence predictable by the Kolmogorov theory:

$$<[n(\mathbf{r}_1 + \mathbf{r}) - n(\mathbf{r}_1)]^2> = C_n^2 \, r^{2/3}$$

where n is the index of refraction, < > means to average over $\mathbf{r}_1$, and $r = |\mathbf{r}|$.

According to a wind tunnel experiment [2], the average phase variation across an optical aperture of 10 cm is about one wave (~0.5 μm). This phase variation can be approximated as

$$\Delta f = [<[n(\mathbf{r}_1 + \mathbf{r}) - n(\mathbf{r}_1)]^2>]^{1/2} \Delta z$$

Using the aperture r = 10 cm and the experimental finding of shear layer thickness Δz = 10 cm [2], $C_n^2 = 5 * 10^{-9}$ $m^{-2/3}$, which is significantly larger than that for natural atmosphere unperturbed by aircraft [13], about 10^{-15} to 10^{-16} $m^{-2/3}$. From C_n^2, r_0 = 2 mm. From v = 200 m/s, f_G = 40 kHz, which shows that the bandwidth of the airborne turbulence is on the order of 100 kHz. Current adaptive optics, however, has a bandwidth of a few kilohertz [4,14].

Despite the complexity of airborne turbulence, some coherent structures may exist inside the shear layer [15]. Because these structures may be dominant in causing large-scale air density fluctuations, we urgently need to understand their temporal and spatial distributions. This knowledge will certainly provide a guide to developing fast adaptive sensors and compensators, the ultimate goals.

OPTICAL NOVELTY FILTER

An optical novelty filter [5] is a high-pass filter that passes rapidly changing input light and rejects slowly changing input light. Many reported novelty filters [6,10,16-18] are in fact time-differential filters. By optically subtracting the current input light from the past, these filters allow only the new features in the input to go to the output. The interval between the current and the past is determined by the filter's response time.

A novelty filter has a finite response time so that it responds to the past input at the current time. The filter is often set up as a self-aligning interferometer [5]. It consists of a beamsplitter at the entrance and a phase-conjugate mirror at the end (see Figure 2). The beamsplitter divides the input light into two copies along two arms, both of them incident on the conjugate mirror.

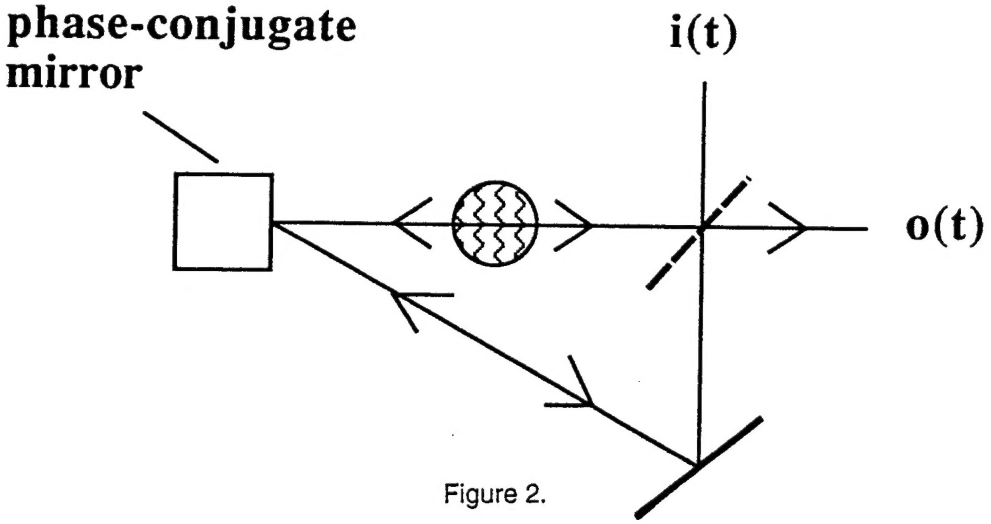

Figure 2.

The phase-conjugate mirror has a finite response time. Instead of reflecting the incident light instantaneously, the mirror first stores the incident light amplitude and phase. After a certain response time, the mirror recalls the memory and retroreflects the incident light with a conjugate phase. The reflected light then retraces the path of the incident light back to the beamsplitter. Because of the conjugate phase, the reflected light cancels all the past distortions caused by the medium and picks up the new phase. Therefore, when it reaches the end, the reflected light contains a time-differential phase distortion of the medium.

In the novelty filter, one arm traverses the phase changing medium and the other arm serves as constant reference. The light waves along the two arms recombine at the beamsplitter and destructively interfere on the exit side [5]. The time-differential phase of the medium is thus presented as the interference signal at the output.

Phase-conjugation has been observed by either stimulated Brillouin scattering or four-wave-mixing [19]. Some well-known materials for four-wave-mixing are photorefractive crystals and Kerr media [20]. Although these materials are highly efficient and easy to use, their response times are tightly constrained by material characteristics, such as diffusion time [21] or relaxation time [22]. Therefore, they cannot provide a flexible response time in accord with the coherence time of turbulence structures.

TIME-DOMAIN STIMULATED PHOTON ECHO

In a three-pulse stimulated photon echo experiment [23], the first two laser pulses burn a persistent spectral hole pattern in the ground state population of a material, such as a rare earth doped crystal at low temperature. After a long waiting time, the third laser pulse excites the material again and stimulates a coherent radiation pulse that is delayed in time. This time delay is equal to the time delay between the first two laser pulses, hence the name echo. In other words, the initial time delay between the first two laser pulses, is memorized by the material and recalled exactly through the echo's timing. This provides the basis of optical memory of temporal modulation.

However, the spectral hole pattern burnt in the material by the first two laser pulses is a spectral hologram. Although not overlapping in time, the two laser pulses overlap in frequency. One laser serves as the object light and the other as the reference [24]. The third laser pulse serves as a reference again to read out the echo as a holographic image of the object. This provides the basis of optical memory of spatial modulation. Therefore, an optical memory can be installed either through temporal modulation of the first or second laser pulse shape, or through spatial modulation of these pulses' intensity or phase profile [8,9].

Spectral hologram needs to be explained. Very narrow spectral holes can be burnt in the absorption spectrum of a rare earth doped crystal at low temperature. This indicates that each rare earth ion has a long coherence time. The spectral holes burnt by the combined first two laser pulses are caused by the interference between them. Although the two laser pulses do not overlap in time, the rare earth ions excited by the first pulse oscillate coherently after that pulse is gone and react to the coming second pulse. Therefore, these ions provide the basis of coherent interference between the two laser pulses. If each laser pulse is weak in intensity, the result of this interference is a second-order spectral modulation of the ions' ground state population. This modulation is a long-lived spectral hole pattern or a spectral hologram.

After a long waiting time, the third laser pulse excites the rare earth ions from this modulated ground state and stimulates their coherent dipole radiations. These ions' radiations become aligned in phase at a delayed time, which is equal to the time delay between the first two laser pulses [23]. Thus the macroscopic radiation reaches maximum at that time in the appearance of an echo pulse.

In general, the echo in the frequency space can be viewed as the linear diffraction of the third laser pulse from the spectral hologram formed by the coherent interference between the first and second laser pulses in a material with narrow homogeneous linewidth:

$$E_e(r,\omega) \sim E_3(r,\omega)\{E_2(r,\omega)[\,E_1(r,\omega)]^*\} \qquad (1)$$

where $E_{1,2,3}(\omega)$ are the amplitudes of the three laser pulses in the frequency space [25], and the bracket { } contains the spectral hologram's amplitude. Eq. (1) is valid for weak laser intensities.

It is then evident that the echo is a conjugate image of $E_1(r,\omega)$ when $E_3(r,\omega)\,E_2(r,\omega)$ is uniform in space, or a real image of $E_2(r,\omega)$ if $E_3(r,\omega)[\,E_1(r,\omega)]^*$ is uniform in space.

PHASE-CONJUGATE REFLECTION

When $E_3(r,\omega)\,E_2(r,\omega)$ is uniform in space, $E_e(r,\omega) \sim [\,E_1(r,\omega)]^*$. The radiation from a material is the complex conjugate of an incident laser. This is the first feature of phase conjugate reflection. The echo is pointed at $\mathbf{k}_e = \mathbf{k}_3 + \mathbf{k}_2 - \mathbf{k}_1$, where $\mathbf{k}_1$, $\mathbf{k}_2$, and $\mathbf{k}_3$ are the wave vectors of the three laser pulses in the nonlinear material. A backward photon echo is established when the second and third laser pulses are antiparallel, i.e., $\mathbf{k}_3 + \mathbf{k}_2 = 0$. Under this condition, $\mathbf{k}_e = -\mathbf{k}_1$. The new radiation pointing as a retroflection of the incident laser is the second feature of phase conjugate reflection. Therefore, the backward photon echo is a phase-conjugate reflection of the first laser pulse. The backward configuration is similar to most four-wave-mixing phase-conjugate-mirrors [22].

However, the photon echo phase-conjugate-mirror (PCM) has a unique character that other PCMs do not have: the arbitrary time delay of its phase-conjugate reflection. The echo is radiated at $t = t_3 + t_2 - t_1$, where t_1, t_2, and t_3 are the incidence times of the three laser pulses in the nonlinear material. From the incidence time of the first laser pulse, the echo is delayed until $(t_2 - t_1)$ after the third laser pulse arrives. Therefore, one can delay the phase-conjugate reflection arbitrarily by delaying the third laser pulse, as long as the spectral hologram is long-lived. Because of the ease of controlling the echo's timing by programming external excitation delay, the photon echo PCM has a very flexible response time. This conveniently suits the study of dynamic phase change on any fast time scale from nanosecond to microsecond.

The reflectivity of the photon echo PCM depends on several parameters. The first laser pulse should be aligned to strike the PCM on the effective area that is pumped by the second and the third laser pulses. If the pump laser pulses have a Gaussian spatial profile, then clearly the

reflectivity at the center of the pumped area is different from the wing. The reflectivity also depends on the time delay between the laser pulses. The delay between the first and second pulses should be shorter than the coherence time of the rare earth ions excited in the PCM. Otherwise, there is no reflectivity because no spectral hologram can be burnt. This requirement is similar to the coherence requirement in conventional holography [26,27].

OUTPUT OF PHOTON ECHO NOVELTY FILTER

In the photon echo novelty filter, the first laser pulse is split by a beamsplitter into two beams along two paths. The two beams are finally incident on the rare earth doped crystal at two $\mathbf{k}_1$ directions (see Figure 3). Because they come along two separate paths, these two beams differ in their incidence direction on the phase-conjugate-mirror. If these two beams strike the same effective area of the phase-conjugate-mirror, the reflectivities for them are the same (assuming they are coincident). Therefore, when either arm of the novelty filter is blocked, we should measure the same echo intensity along the other arm at the output of the filter because the two arms are symmetric about the beamsplitter. That is, the light on either arm experiences one reflection and one transmission at the beamsplitter to go from the input to the output of the filter.

If the echo along one arm sees a new phase change of δ while the other arm remains constant, the output of the novelty filter (channel y) is

$$I(y) = 2(1 - \cos\delta)I(e) \tag{2}$$

where I(e) is the output when either arm is blocked. Here we assume that the two $\mathbf{k}_1$'s have no cross talk in the nonlinear crystal so that blocking one does not affect the other. This is true when both two $\mathbf{k}_1$'s are weak in intensity so that their combination in the crystal is also weak in intensity.

Using Eq. (2), we can find δ by measuring I(y) and I(e). These measurements are not done at the same time because one arm needs to be blocked to measure I(e). To find δ without measuring I(e), we refer to the monotony output [5] at the beamsplitter. This output is the recombined echo that goes back to the light source. Because the monotony output is also proportional to I(e), we can find δ by measuring the novelty (channel y) and the monotony (channel x) output at the same time:

$$I(y)/I(x) = (1- \cos\delta)/(p + q \cos\delta) \tag{3}$$

where p and q are constants defined in appendix A.

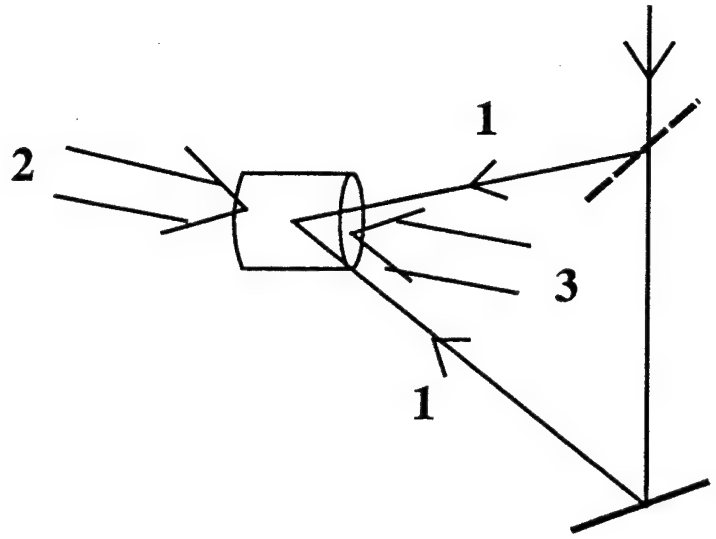

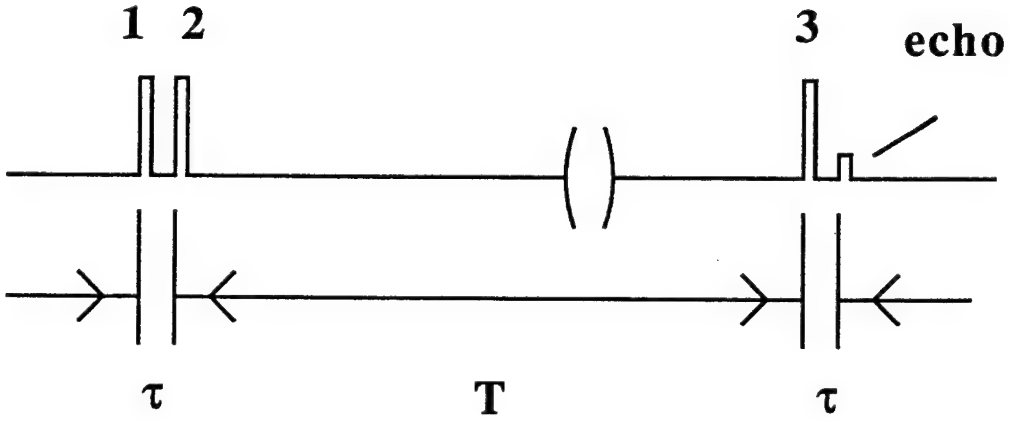

Figure 3.

EXPERIMENTAL CONDITION

PROOF OF CONCEPT ON NANOSECOND TIME SCALE

The laser pulses for the experiment were produced by a dye laser (SpectraPhysics PDL-1) pumped by the second harmonic of a Q-switched Nd:YAG laser (Quanta Ray DCR-1). Running at 10 Hz repetition rate, the laser pulse was 7 ns in duration, 6 GHz in bandwidth, and 580 nm in wavelength. This wavelength was tuned to excite the $^7F_0$-$^5D_0$ transition of a Eu-doped crystal that was used for the phase-conjugate-mirror. The laser was linearly polarized by a Glan prism.

The laser pulse was split into three pulses at times t_1, t_2, and t_3 (see Figure 4). A white cell introduced delays of about 24 ns and 114 ns for $t_2 - t_1$ and $t_3 - t_1$, respectively. The first laser pulse was split into two copies that were both focused to 0.2 mm on the europium crystal. They were almost coincident. The second and the third laser pulses were spatially filtered and collimated. They were aligned to overlap and counterpropagate through the europium crystal with the same beam diameter of 1 mm. The angle between either $\mathbf{k}_1$ and $\mathbf{k}_3$ was about 50 mrad. When the intensity of any one of three laser pulses was attenuated by 50%, the echo intensity also dropped by 50%. This indicated that the laser intensity is weak enough.

The europium doped crystal is 0.1% Eu^{3+}:Y_2SiO_5 (Scientific Materials), which is 8 mm in diameter and 7 mm long. It was mounted in a closed-cycle refrigerator (RMC model 22). The temperature was kept at 19-20 K. This temperature was the lowest point to remove the accumulated photon echo from the crystal [28]. All the echo data were taken at site 2 of the crystal [29]. The optical density of our crystal at site 2 was less than one.

An avalanche transistor driver provided microsecond-long high voltage pulses to a Pockels cell (KD*P) installed along one arm of the novelty filter. The KD*P crystal generates a phase modulation pulse that is linearly proportional to the high voltage pulse. The KD*P crystal's response time is a few nanoseconds. The phase modulation pulse has a rise time of a few nanoseconds and a length of a few microseconds. This pulse was seen as a step function by the nanosecond light pulses. The beginning time of the high voltage pulse was after the first laser pulse but before the echo. To use the KD*P as a pure phase modulator, we aligned one of its extinction axes parallel to the laser's linear polarization.

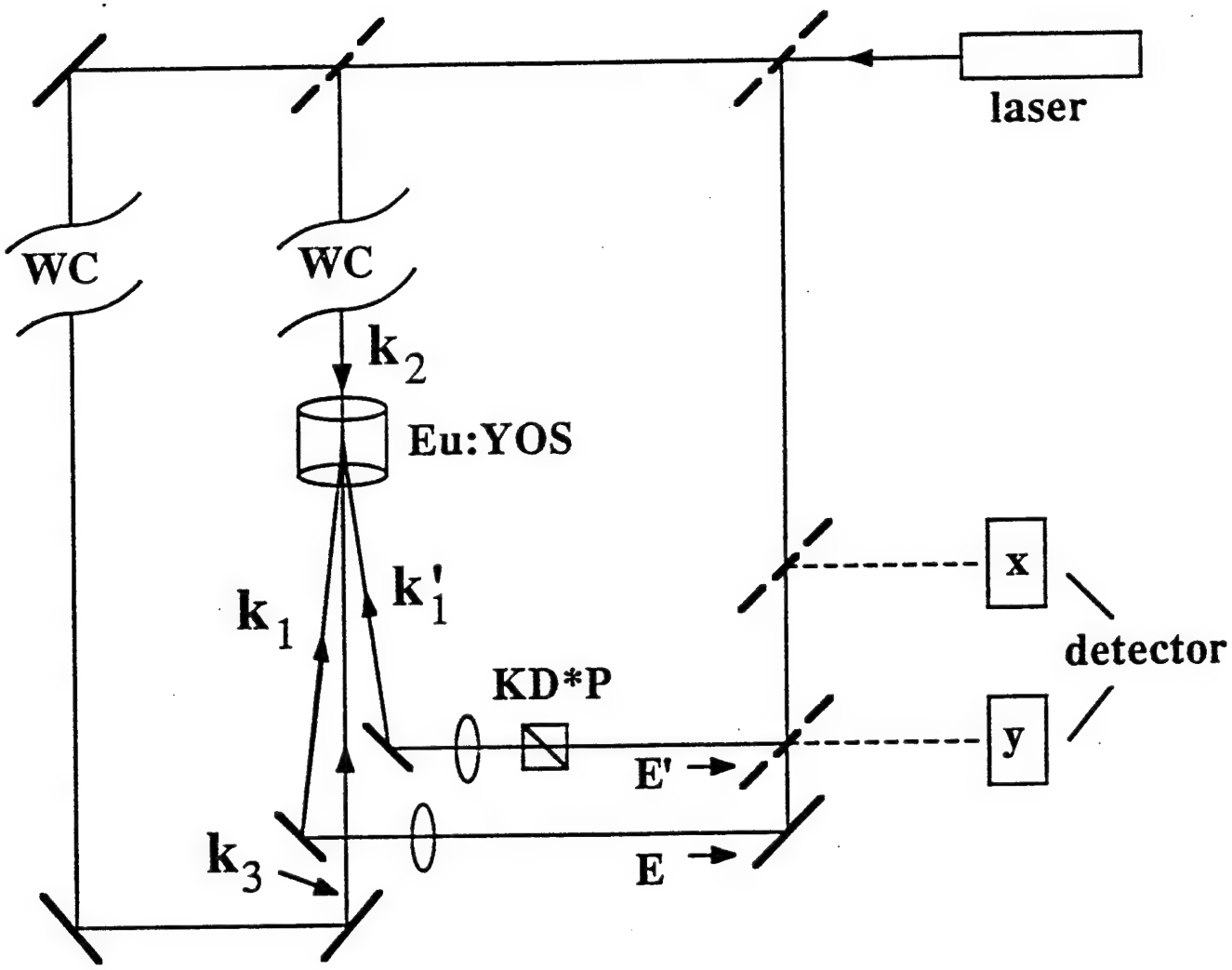

Figure 4.

The phase modulations (δ) along the two extinction axes of KD*P are equal but opposite in sign [30]. To calibrate δ, we aligned the extinction axes at exactly 45° from the laser's polarization. The beginning time of the high voltage pulse was changed to be before the first laser pulse. We measured the output intensity of the Pockels cell after a cross polarizer. In this configuration, $I_O = I_i(\sin\delta)^2$, where I_i and I_O were the input and output intensity, respectively. Thus δ was calibrated. The maximum phase modulation in one single KD*P was less than 90°. When we wanted a modulation more than 90°, we used two KD*P crystals in series.

We tested the filter's output under several δ values. We varied δ in two ways. First, we varied it among a set of discrete values by connecting cables of different lengths to the avalanche transistor driver output. This changed the capacitive load to the driver and amplitude of the high voltage pulse. Second, the driver electronics was modified to shorten the high voltage pulse to 100 ns. In this way, the phase modulation seen by the echo was varied by shifting the beginning time of the high voltage pulse relative to the echo. Thus the echo saw a different amplitude of phase change along the 100-ns-long pulse. To prevent the first laser pulse from also seeing the phase change, the high voltage pulse had to be shorter than $t_e - t_1$, where t_e and t_1 were the time of the echo and the first laser pulse, respectively.

A light switch consisting of a Pockels cell and two cross polarizers was installed to remove the laser scattering from the echo at the output. The echo was first detected by a CCD camera. We aligned the two $\mathbf{k}_1$'s to achieve a Gaussian spatial profile for the echoes and to minimize the background when the echoes canceled each other. The echoes at channel y and x were then detected by fast photodiodes. The average echo gave a voltage pulse of about 100 mV in the photodiode. The maximum echo was about 10 times larger in intensity. The output of the photodiodes was integrated by boxcar integrators and then digitized by an A/D board in a PC.

TEST OF PERFORMANCE ON MICROSECOND TIME SCALE

We used two Q-switched Nd:YAG lasers to pump two pulsed dye lasers. The dye lasers had 7-ns pulse duration, 6-GHz bandwidth, and 10-Hz repetition rate. One dye laser provided both the first and second laser pulses, which were optically separated by 20 ns. The other dye laser provided the third laser pulse, which could be continuously delayed from the first dye laser (see Figure 5). We chose either Eu^{3+}:Y_2SiO_5 (8-mm diameter, 7-mm thickness) or Pr^{3+}:Y_2SiO_5 (8-mm diameter, 2-mm thickness) as the nonlinear material for photon echo. The Eu and Pr crystals were held at 18 and 9 K, respectively, in a closed cycle refrigerator. At these temperatures, the accumulated photon echoes vanished in these crystals.

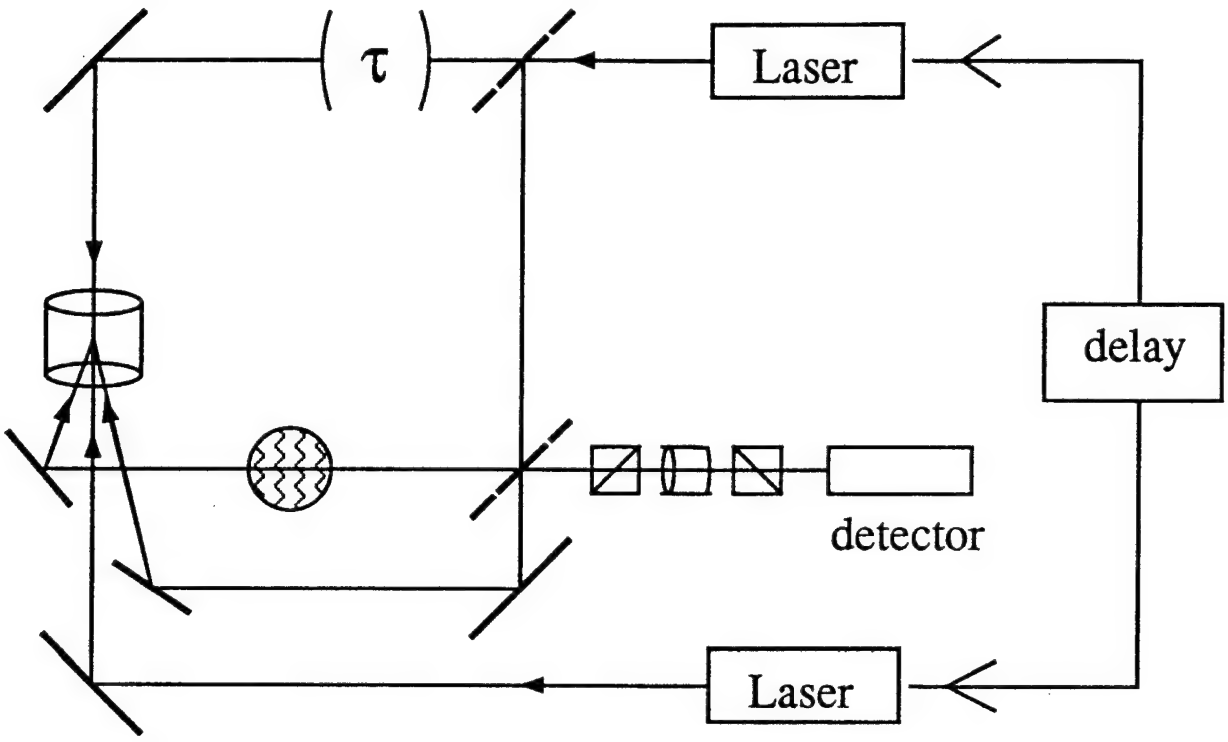

Figure 5.

The dye lasers were tuned to excite either the $^7F_0$-$^5D_0$ transition of Eu^{3+}:Y_2SiO_5 or the $^3H_4$-$^1D_2$ transition of Pr^{3+}:Y_2SiO_5. Because there are two sites in the Y_2SiO_5, the two lasers were tuned to excite the rare earth ions at the same site. We used site 2 for Eu and site 1 for Pr to take advantage of the ions' larger oscillator strengths at these sites [31,32]. The inhomogeneous linewidths of Eu and Pr at these sites were measured to be 11 and 49 GHz (broadened by the 6-GHz laser bandwidth), respectively. The peak absorptions of the laser in our Eu and Pr doped crystals were 18% and 70%, respectively.

Because Pr has about ten times greater oscillator strength than Eu, the echo signal from Pr doped crystal was much larger. However, the laser intensity could also be too high for Pr because of its large oscillator strength. A strong incidence laser intensity could violate the condition of phase-conjugate-reflection. In our experiments, we did not focus the first laser pulse on the Pr doped crystal. In this way we prevented the laser intensity from going too high. For both the Eu and Pr doped crystals, the optimized echo signal was bright enough to be seen and gave more than 1 V of response on fast photodiodes.

Two transparent media that can generate phase changes were used to test the novelty filter. The first medium was a KD*P crystal to which we supplied microsecond-long high voltage pulses. The beginning time of the high voltage pulse was fixed relative to the first two

laser pulses from one dye laser. The third laser pulse (from the other dye laser) was scanned in time relative to the high voltage pulse. In this way, the echo was scanned across the microsecond-long pulse of phase change.

The second medium was a helium jet. Compressed helium gas was ejected vertically from a 2-mm-diameter round nozzle at a speed about 100 m/s. The horizontal laser beam intersected the jet above the nozzle. We selected helium because it has a very different index of refraction from air (at standard temperature and pressure, n(He) = 1.000036, n(air) = 1.000293). Therefore, a small change in the helium jet thickness can induce a large change in the optical path length (a 1-mm change in helium thickness gives about 0.25-μm change in optical path length). We first used fast photodiodes to spatially integrate the echo intensity through the jet. When the helium jet needed to be spatially resolved, it was first imaged on the crystal, using the first laser pulse, and then imaged on a CCD camera, using the echo.

RESULTS AND DISCUSSION

PROOF OF CONCEPT ON NANOSECOND TIME SCALE

Data for Novelty Filter Alone

The value of δ (novelty filter) was calculated from $I(y) = 2(1 - \cos\delta)I(e)$. For each measurement of I(e) and I(y), we took 500 laser shots and averaged the signal. I(e) was measured separately along the two arms, and we checked that they did not differ more than 10%. The average of I(e) along the two arms was used in the calculation. We repeated this procedure 5 times and averaged the result to get the final value of δ. $\sigma(\delta)$ is the standard deviation of δ from the average in these 5 measurements.

δ (calibrated) was calculated from $I_o = I_i(\sin\delta)^2$. The error in calibration was assumed to be negligible. The results are given below.

δ (Calibrated)	δ (Novelty Filter)	Error	$\sigma(\delta)$ (Novelty Filter)
144°	137°	-7°	6°
128°	117°	-11°	2°
109°	107°	-2°	2°
74°	71°	-3°	3°
57°	60°	3°	1°
35°	46°	11°	1°
0°	15°	15°	

Data for Novelty Filter with Monotony Reference

The value of δ (novelty filter) was calculated from $I(y)/I(x) = (1 - \cos\delta)/(p + q\cos\delta)$. p and q needed to be measured only once (see Appendix A). We measured I(y)/I(x) for 100 laser shots and averaged them to calculate the final value of δ. δ can also be calculated from I(y)/I(x) on single-shot basis. $\sigma(\delta)$ is the standard deviation of the single-shot δ values in these 100 shots from the final δ, as given below.

δ (Calibrated)	δ (Novelty Filter)	Error	σ(δ) (Novelty Filter)
86°	85°	-1°	5°
82°	81°	-1°	5°
78°	72°	-6°	5°
73°	71°	-2°	6°
61°	59°	-2°	6°
53°	57°	4°	6°
43°	43°	0°	6°
38°	41°	3°	5°
34°	38°	4°	5°
0°	20°	20°	6°

Data for Fast Phase Modulation (Novelty Filter with Monotony Reference)

In our measurement of δ (novelty filter), we scanned the phase modulation by shifting its time (relative to the laser) stepwise with 1-ns step sizes. At each step, we took 10 laser shots and found I(y)/I(x) through a linear fit. After the whole scan, we got a curve of I(y)/I(x). This procedure was repeated 10 times and the resulting 10 curves were averaged to get a final curve. From this curve of I(y)/I(x) we calculated a curve of δ (novelty filter), as shown in Figure 6.

The phase modulation pulse was scanned in a similar manner during calibration. In the measurement of δ (novelty filter) and δ (calibration), the fast phase modulation was applied to the echo and the first laser pulse, respectively. To compare the two measured curves of δ, we estimated the time interval between the echo and the first laser pulse. We shifted the time axis of one curve of δ with respect to the other and got a reasonably good fit, as shown in Figure 6.

Discussion

From the data, we consistently saw a background signal that gave a false measurement of δ of 15°-20°. This was the result of the incomplete cancellation of the two echoes at the output when no phase modulation was applied. This incomplete cancellation could happen because the two echoes at the output were not exactly equal in intensity. However, the two echoes did not differ more than 10% in intensity in our experiment. This small intensity difference would not give a background in δ more than 3°. Therefore, the main cause of background is that the two echoes are not 180° out of phase.

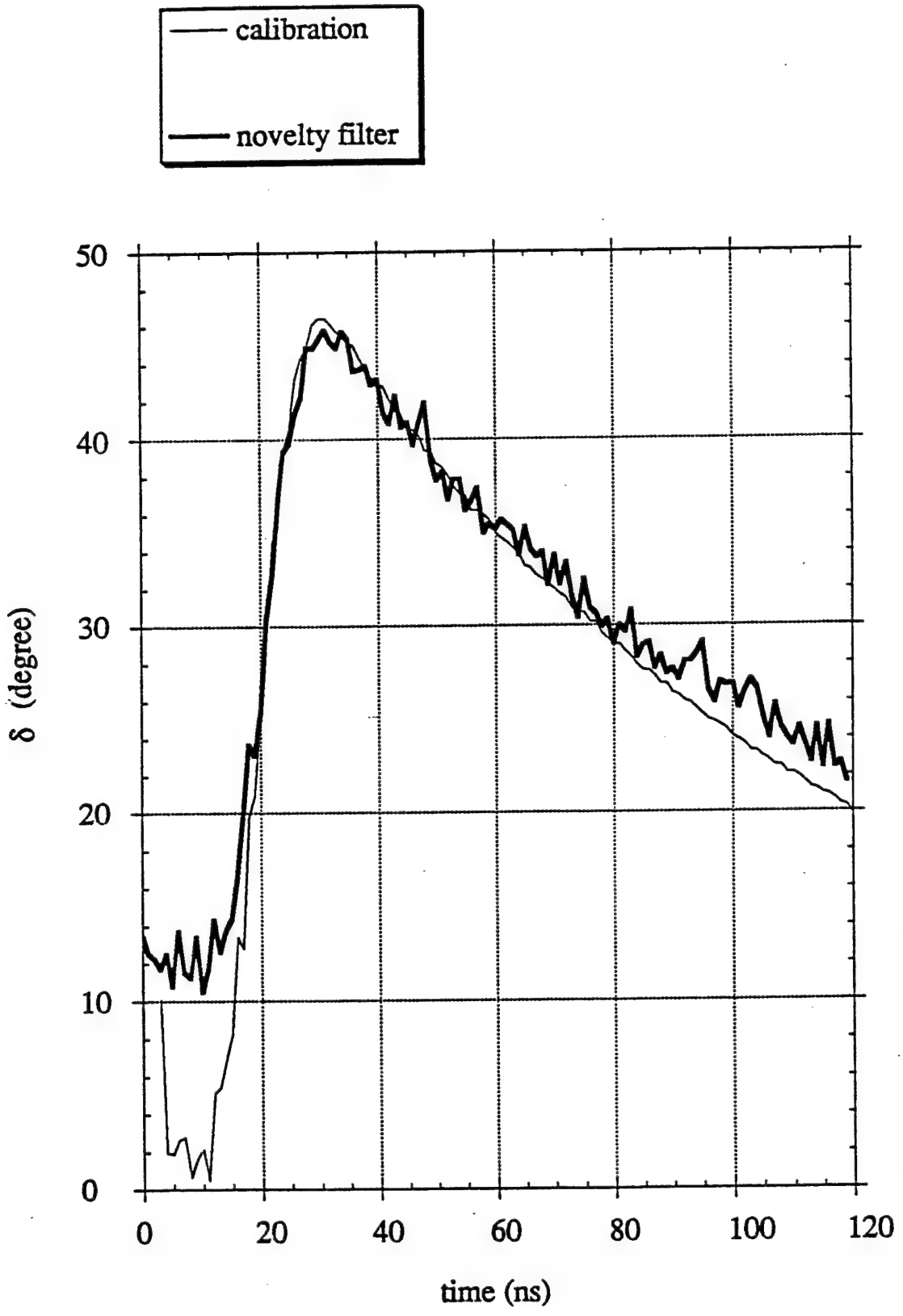
calibration
novelty filter
50
40
30
20
10
0
δ (degree)
0
20
40
60
80
100
120
time (ns)

Figure 6.

One explanation was that the beam divergences of $\mathbf{k}_{2,3}$ were not zero due to diffraction. Since $\mathbf{k}_2 + \mathbf{k}_3$ had some deviation around zero, $\mathbf{k}_e$ also had some deviation around $-\mathbf{k}_1$. This affected the phase-conjugate reflection from canceling the phase of input laser. However, because $\mathbf{k}_{2,3}$ are 1-2 mm in diameter and $\mathbf{k}_1$ is 0.2 mm, we found that diffraction-limited beam divergence would not give a background of δ more than 2°.

The background could also be affected by how flat the wavefronts of $\mathbf{k}_{2,3}$ were as well as by how flat the rare earth crystal surface was. We found that the background was quite sensitive to these conditions. The background of δ of 15°-20° seen in our experiment could be suppressed to about 10° by polishing the crystal surface to higher degree. The remaining cause of the background needs further investigation.

TEST OF PERFORMANCE ON MICROSECOND TIME SCALE

Single-Pixel Phase Modulator

We scanned the time of the third laser pulse (relative to the phase modulation pulse) stepwise, with one step for each single laser shot. The data are shown in Figure 7 together with the calibration data. We shifted the time axis of one curve of δ with respect to the other and got a reasonably good fit, as shown in Figure 7.

In Figure 7, the data preceding the rising edge was the background, which is about 0.025 wavelength (~0.6 μm), or 9°. The accuracy of the novelty filter was 0.02 wavelength and the resolution was also about 0.02 wavelength, or 7°.

Real Turbulent Jet

The data are shown in Figures 8 and 9. We used Eu doped crystal for these measurements. First, we turned off the jet and measured the background over a long response time (see the lower parts of Figures 8 and 9). When the response time was increased from 20 to 200 μs, the background clearly rose. It was 0.04 wavelength at 100 μs and 0.08 wavelength at 200 μs. We attribute this rise of background to slow phase modulations along the optical path caused by the environment. These slow perturbations were rejected by the novelty filter under short response times. When the response time was lengthened, the filter relaxed to lower cutoff frequency. As a result, more slow perturbations leaked through the filter.

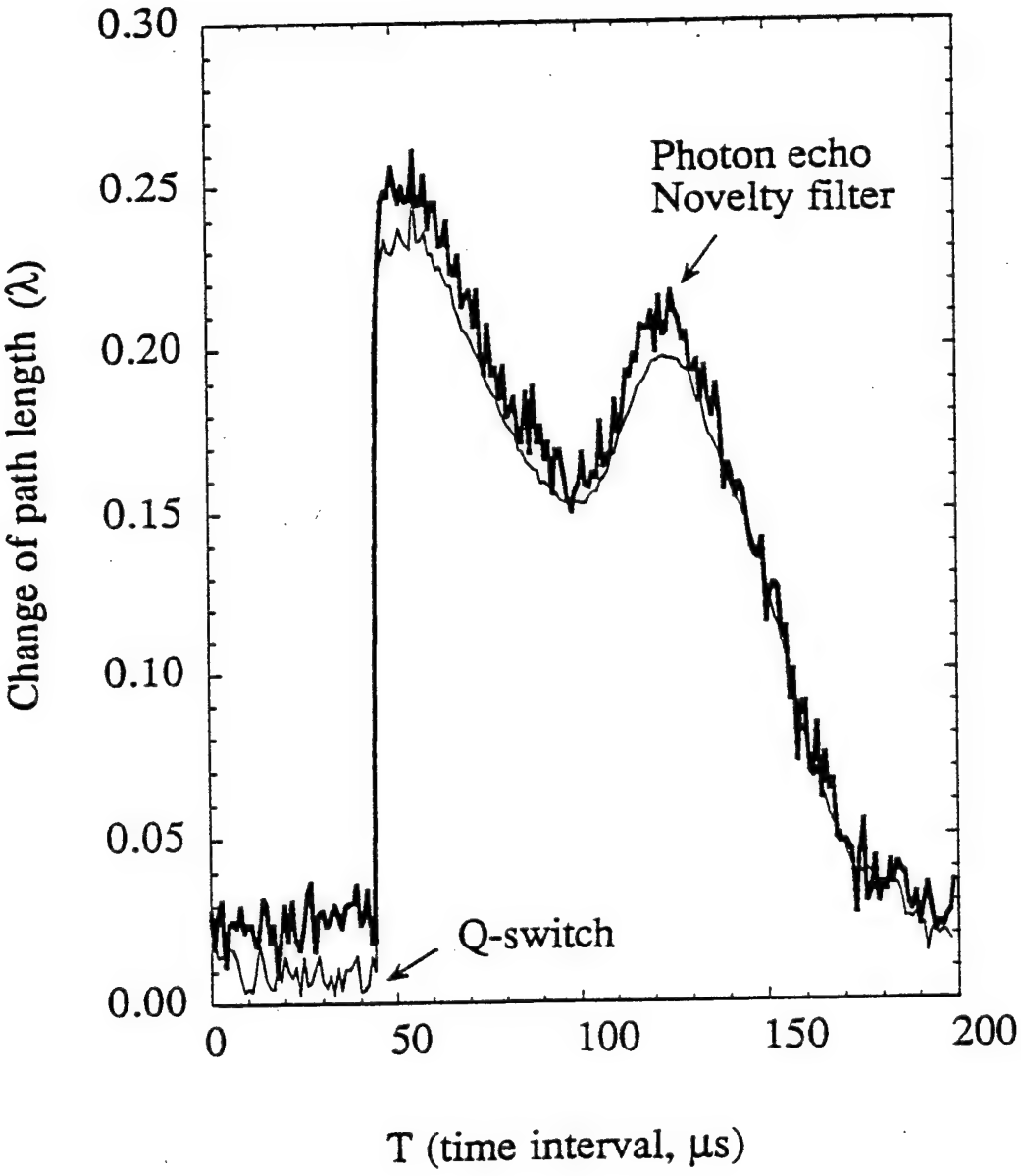
0.30
0.25
0.20
0.15
0.10
0.05
0.00
Change of path length (λ)
Photon echo
Novelty filter
Q-switch
0
50
100
150
200
T (time interval, μs)

Figure 7.

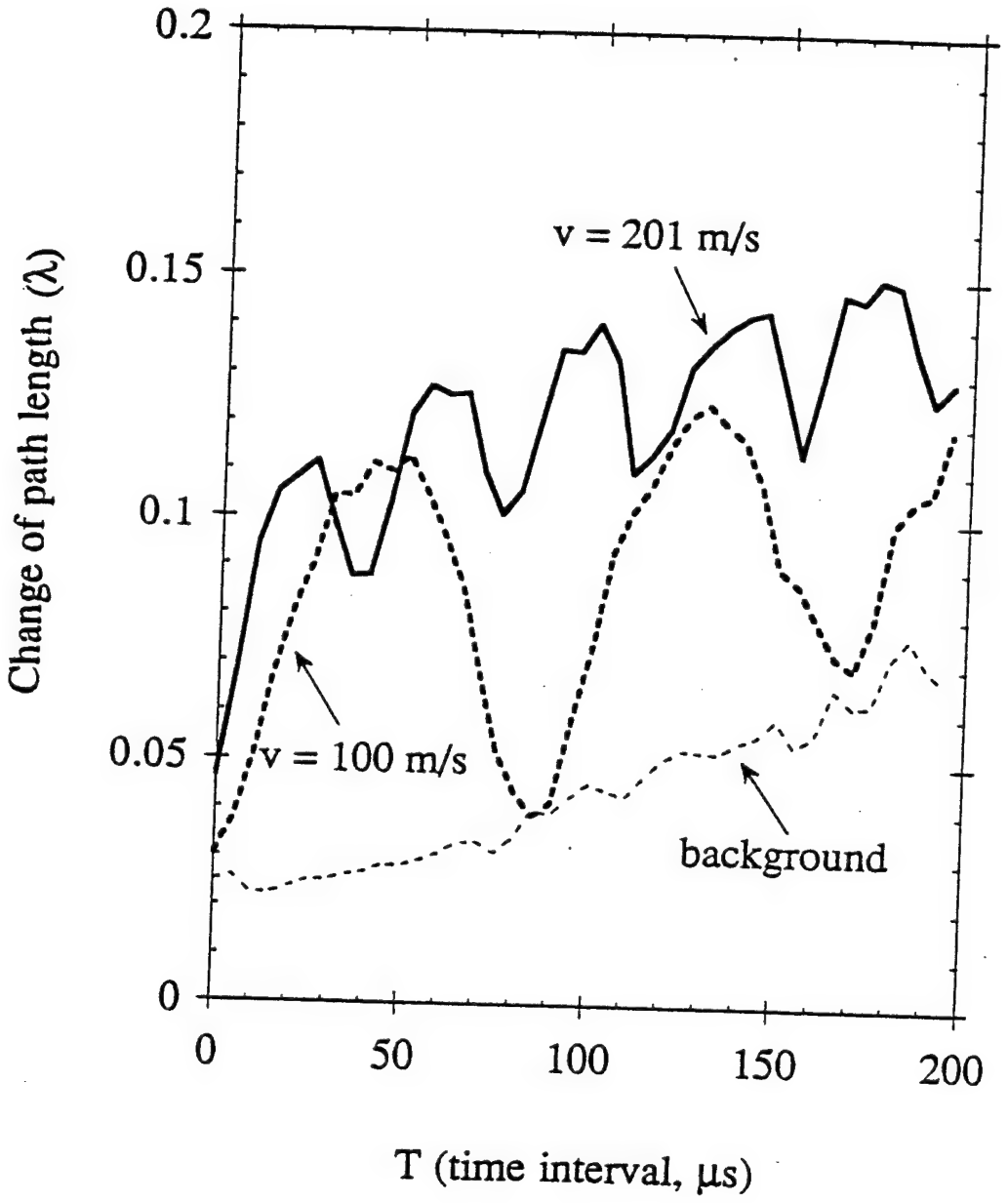
0.2
0.15
0.1
0.05
0
Change of path length (λ)
v = 201 m/s
v = 100 m/s
background
0
50
100
150
200
T (time interval, μs)

Figure 8.

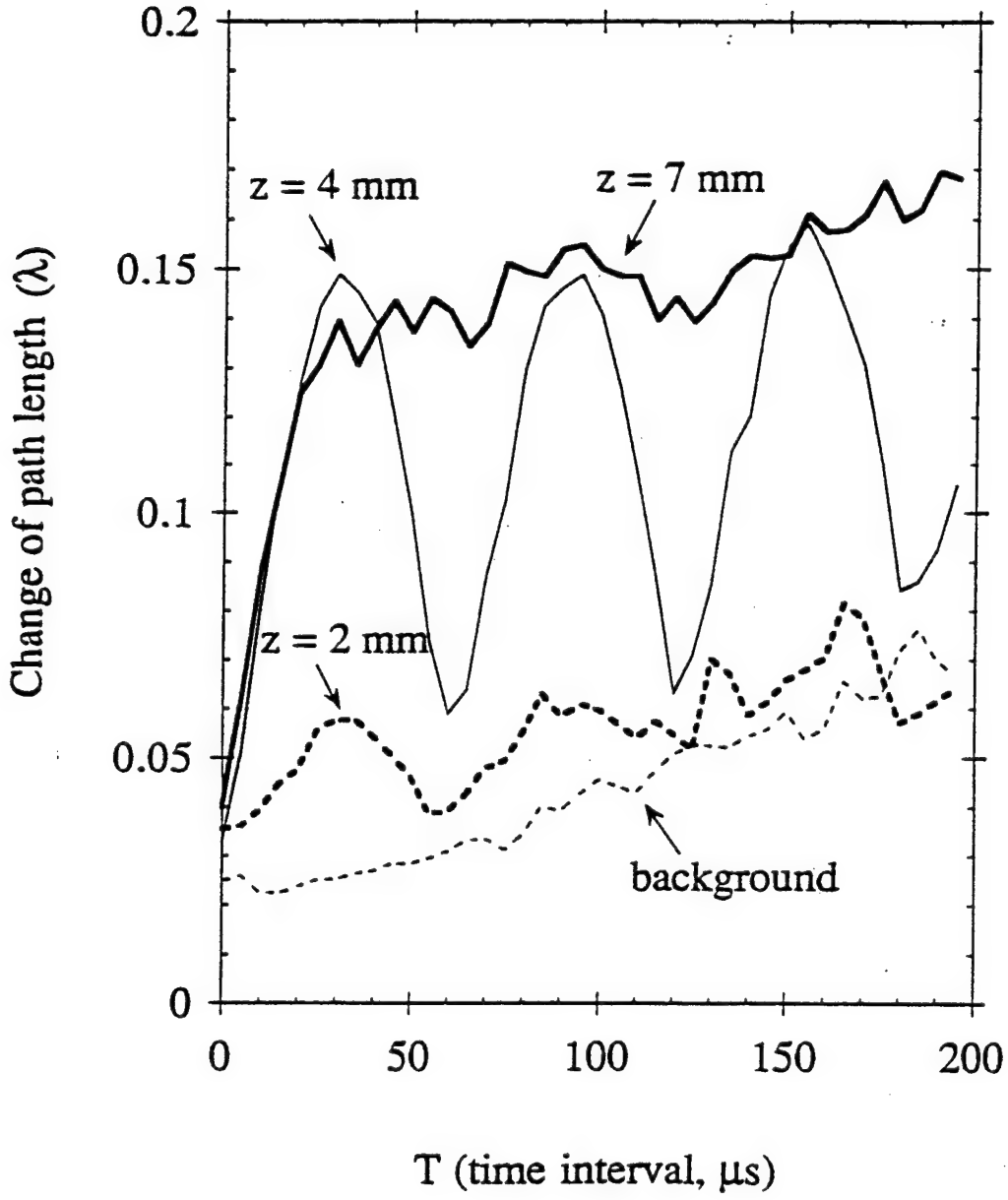
0.2
0.15
0.1
0.05
0
0
50
100
150
200
z = 4 mm
z = 7 mm
z = 2 mm
background
Change of path length (λ)
T (time interval, μs)

Figure 9.

When the helium jet was turned on, the phase distortion was a continuous and random event in time. However, the novelty filter was limited to 10-Hz sampling frequency by the laser's repetition rate. Each data point in Figures 8 and 9 was taken from the average of 100 sampling measurements. The response time of the filter was then changed to go to the next point.

When the laser crossed the jet at 4 mm above the nozzle, an unexpected sinusoidal oscillation appeared in the novelty output as we scanned the filter's response time (see Figure 8). The oscillation frequency was about 10 kHz and increased at higher jet speed. We believe this oscillation is caused by the jet's acoustic vibration, which caused the jet thickness to change periodically and induced oscillation in the optical path length. Although the 10-kHz vibration was sampled at 10 Hz by the laser, the periodic oscillation can be observed by averaging the novelty output. This average is derived in Appendix B.

The jet's acoustic vibration was proved by detecting the jet's whistle and Fourier transforming the audio signal. We got the same oscillation frequency shown in the novelty filter output. This acoustic vibration is an "edge tone" of the jet [33]. Its frequency can be estimated by the ratio of the jet speed to the nozzle diameter. Using a jet speed of 100 m/s and a nozzle diameter of 2 mm, we get 50 kHz, which is on the order of the observed frequency.

The phase change was quite small near the nozzle (see Figure 9) because the jet in that region was laminar and changing slowly in time. The optical path length was almost constant there. Further away from the nozzle, the phase change increased dramatically, indicating that the jet in that region was turbulent and changing rapidly in time. In Figures 8 and 9, the phase changes rose to asymptotic levels within 20-40 μs. The rise time was shorter at higher jet speed: 40, 30, and 20 μs at jet speeds of 100, 130, and 200 m/s. These data indicated that the inverse of the rise time was linear to the jet speed. This result is consistent with the Greenwood frequency [12] mentioned above. As a simulation of airborne turbulence, the helium jet showed that the phase distortions do change with a bandwidth of about 40 kHz.

In the measurements of the jet's spatial structures, we used Pr-doped crystal. Because the jet is a nonuniform phase screen, the laser passing through it and going to the crystal directly would be highly distorted at the crystal surface. As a result, the laser would not strike the effective area of the crystal properly. This would affect the phase-conjugate reflection. To solve this problem, we imaged the jet on the crystal using the laser. This image was expected to be uniform in intensity, because the jet was illuminated to be a phase-only object with no amplitude modulation.

After we imaged the jet on the crystal, when the novelty filter response time was 100 ns, we found that the echo coming back through the jet maintained a uniform profile at far field. This proved the effectiveness of the imaging. The jet also showed no phase change over a short time of 100 ns. This result indicated there was no faster dynamics in the turbulent jet.

To resolve the phase change on a microsecond time scale, we lengthened the response time of the novelty filter into a 10-μs region. The echo returned and illuminated the jet to be a phase-only object that contained a profile of the phase change over the response time. The jet was then imaged on a CCD camera using the echo.

This "phase-only" image is shown in Figure 10 by its intensity profile. We found that the image was not scattered and nearly uniform in intensity. Inside the image were some nonuniform structures, probably caused by some high spatial frequencies lost in the imaging. To transform the phase-only image to an intensity profile, the echo carrying the image was interfered with the reference echo. The resulting interference is shown in Figure 11. These data showed the intensity of the phase change over a time of 20 μs.

We also imaged the phase change over a time of 2 μs (data not shown) and observed much weaker novelty signal by the interference (the turbulence had barely evolved within 2 μs.) We finally translated the jet in x and y directions transverse to the z direction of the laser beam, and we were able to observe the variations of the phase change structure in different regions of the jet.

ADVANTAGES AND LIMITATIONS OF THE PHOTON ECHO NOVELTY FILTER

The photon echo novelty filter has several limitations. So far, the best sensitivity of photon echo novelty filter to phase change is 0.025 wavelength. This low sensitivity is inferior to the Shack-Hartmann wavefront slope sensor, which has a sensitivity of 0.0006 wavelength [14]. The novelty filter has no sensitivity to the sign of phase change, which means it cannot tell a positive phase change from negative change, because the novelty filter measures $\cos\delta$. The sinusoidal nature of $\cos\delta$ also introduces uncertainty to the absolute value of δ when δ exceeds 0.5 wavelength.

The photon echo novelty filter can be compared with the traditional double-pulse holographic interferometer [26,27]. In the latter, the phase distortions are recorded twice at two consecutive moments in the same holographic film. After the film is developed, the two holograms are read out simultaneously and their interference shows the time-differential phase change. Therefore, the photon echo novelty filter and the double-pulse holography detect the same change in phase.

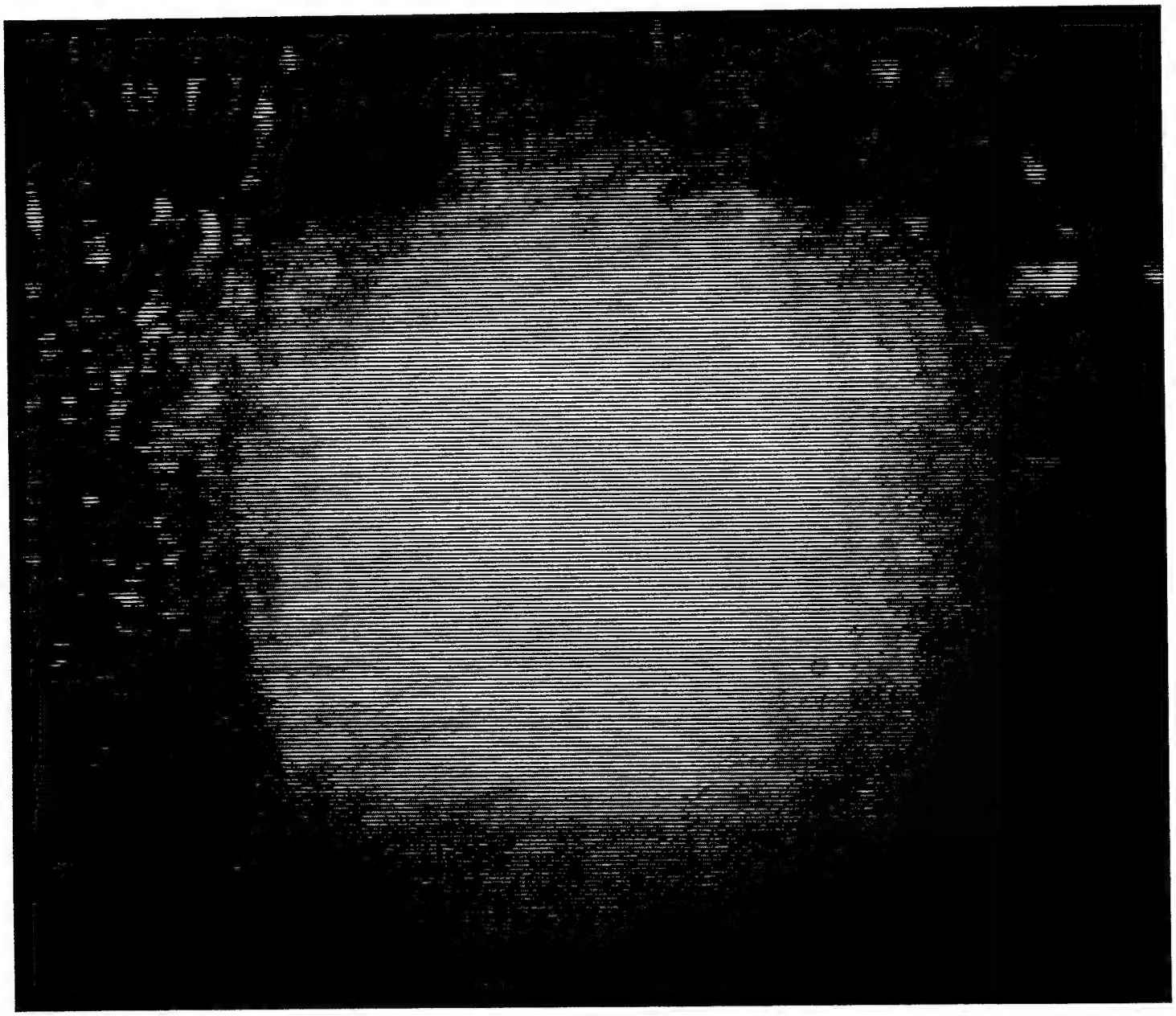

Figure 10.

Figure 11.

The key difference between the two techniques is whether the time-differentiation of phase happens in real time. The photon echo novelty filter needs to record only one phase map at the first moment. This phase map is immediately read out at the second moment and the time-differentiation is finished in real time. This is a great advantage of novelty filter over double-pulse holography.

The two techniques are different in their data representations. The photon echo novelty filter gives a map of the intensity of phase change with zero background. In contrast, the double-pulse interferometer gives a map of straight fringes as background. The amplitude of phase change can be measured from the distortion of these straight fringes [2,3]. Because it does not measure $\cos\delta$ but δ directly, the double-pulse holography has an advantage over novelty filter.

Finally, the photon echo novelty filter is based on inefficient third-order nonlinear radiations. The filter requires high power lasers and cryogenic cooling of the nonlinear crystal. These are drawbacks compared with double-pulse holography.

CONCLUSIONS AND RECOMMENDATIONS

In summary, we have designed the setup, demonstrated the concept, and tested the performance of the photon echo novelty filter to measure a fast change in phase distortion. The filter's sensitivity is better than 0.05 wavelength (~0.6 μm) under a response time of <20 μs. Its accuracy and resolution are both approximately 0.02 wavelength. The filter is proved to be able to follow and resolve a fast phase change event on airborne turbulence time scale. This novelty filter can now be applied to probing a table-top real turbulent flow that simulates airborne turbulence. We showed that the filter can resolve the coherent temporal structures in the flow. Spatial resolution of the filter was also tested.

In the future, we wish to investigate several issues. First , we have so far proved that the time-domain-stimulated photon echo can record and recall a phase-only map through phase-conjugate recall. In other words, we have proved that the recalled phase map exactly cancels the original phase modulation. It would be helpful to provide additional proofs of the phase-only memory by two methods. One method is to recall the conjugate phase map, but not let it return through the original phase modulator. Instead, we can use a beamsplitter to direct it to a Hartmann wavefront sensor and read it out. In this way, we can have a direct comparison of the recalled conjugate phase map and the original one. The second method is to recall the memory in the forward echo rather than the backward phase-conjugate echo. To do this, we need to let the second laser pulse (instead of the first pulse) in the echo experiment carry the phase modulation. We also need to let the first and third laser pulses be colinear, i.e., $\mathbf{k}_1 = \mathbf{k}_3$. In this way, $\mathbf{k}_e = \mathbf{k}_2$. We can thus direct the echo to a Hartmann sensor, read it out, and compare it with the original one.

SRI International has been leading the state-of-art in amplitude-only bitmap memory [24]. Based on our understanding of the basic physics and our expertise on the technology, we believe a forward echo experiment will give a definitive proof of the phase-only memory in hole-burning materials. We would like to conduct such an experiment using the turbulent helium jet. By directing a copy of the laser carrying the original random phase modulation and the echo carrying the recalled phase into a Hartmann sensor, we will be able to have a direct measurement of error rate.

We also propose to apply the photon echo novelty filter to tracking the temporal structure of fast phase change in real time. To do this, we need to sample the phase change rapidly throughout the entire coherent time of turbulence. We would like to acquire a laser source with

high repetition rate (preferably 100 kHz), although the train of laser pulses need not last longer than the coherent time of turbulence. The laser should be able to tune on resonance with certain transition of rare earth ions.

We need to modify the novelty filter so that it can discern positive phase changes from negative ones. One solution is to install a fast beam deflector in the reference arm of the novelty filter. This beam deflector should be able to provide a sudden and small transverse shift to $\mathbf{k}_e$ along the reference arm. As a result, the two echoes interfering at the output will show straight fringes as background. This will allow a direct measurement of δ.

To put the novelty filter on a plane and probe real airborne turbulence, the laser beam diameter in the filter needs to be expanded to about 100 mm to suit the turbulence's spatial scale [2,3]. Therefore, a telescope setup to expand the beam and a turbulent jet with 100 mm cross section are needed in future table top experiments.

Finally, we want to suppress the background of the filter to a much lower level. We have already proved that flattening the second and third laser pulses' wavefront and polishing the rare earth crystal surface give a better phase-conjugate-mirror. Reducing the environmental perturbations also helps to reduce the background. We want to find out how much background is related to the intensity of the first laser pulse and its alignment of incidence on the rare earth crystal. This knowledge may help reduce the background even more.

REFERENCES

1. K. G. Gilbert and L. J. Otten, Eds., *Aero-Optical Phenomena,* Vol. 80, Progress in Astronautics and Aeronautics (AIAA, New York, 1982), pp. 1-9.

2. W. C. Rose, "Nearfield Aerodynamics and Optical Propagation Characteristics of a Large-Scale Turret Model, " AFWL TR-81-28, Air Force Weapons Laboratory, Kirtland AFB, NM (February 1982).

3. J. E. Craig and W. C. Rose, "The Optics of Aircraft Shear Flows," Proc. AIAA Shear Flow Control Conference, AIAA-85-0557, AIAA (March 1985).

4. R. Q. Fugate, B. L. Ellerbroek, C. H. Higgins, M. P. Jelonek, W. J. Lange, A. C. Slavin, W. J. Wild, D. M. Winker, J. M. Wynia, J. M. Spinhirne, B. R. Boeke, R. E. Ruane, J. F. Moroney, M. D. Oliker, D. W. Swindle, and R. A. Cleis, "Two Generations of Laser-Guide-Star Adaptive-Optics Experiments at the Starfire Optical Range," J. Opt. Soc. Am. A **11**, 310-324 (1994).

5. D. Z. Anderson and J. Feinberg, "Optical Novelty Filter," IEEE J. Quantum Electron. **25**, 635-647 (1989).

6. D. Z. Anderson, D. M. Lininger, and J. Feinberg, "Optical Tracking Novelty Filter," Opt. Lett. **12**, 123-125 (1987).

7. M. K. Kim and R. Kachru, "Long-Term Image Storage and Phase Conjugation by a Backward-Stimulated Echo in Pr^{3+}:LaF_3," J. Opt. Soc. Am. B **4**, 305-308 (1987).

8. X. A. Shen, E. Chiang, and R. Kachru, "Time-Domain Holographic Image Storage," Opt. Lett. **19,** 1246-1248 (1994).

9. X. A. Shen and R. Kachru, "Time-Domain Optical Memory for Image Storage and High-Speed Image Processing," Appl. Opt. **32**, 5810-5815 (1993).

10. Y. Zhang and R. Kachru, "Photon Echo Novelty Filter for Measuring a Sudden Change in Index of Refraction," Appl. Opt. **35**, 6762-6766 (1996).

11. Y. Zhang and R. Kachru, "Photon Novelty Filter: A Unique Time-Differential Sensor of Optical Wavefront Distortion Caused by Airborne Turbulence," Appl. Opt., to be published.

12. M. C. Roggemann, B. M. Welsh, and R. Q. Fugate, "Improving the Resolution of Ground-Based Telescopes, " Rev. Mod. Phys. **69**, 437-505 (1997).

13. R. K. Tyson, *Principles of Adaptive Optics* (Academic, Boston, 1991), pp. 36.

14. L. McMackin, B. Masson, N. Clark, K. Bishop, R. Pierson, and E. Chen, "Hartmann Wave Front Sensor Studies of Dynamic Organized Structure in Flow Fields," AIAA **33**, 2158-2164 (1995).

15. U. Frisch, *Turbulence, the Legacy of A. N. Kolmogorov* (Cambridge University, Cambridge, 1995), pp. 108.

16. J. Khoury, C. L. Woods, and M. Cronin-Golomb, "Photorefractive Holographic Interference Novelty Filter," Opt. Commun. **82**, 533-538 (1991).

17. F.T.S. Yu, S. Wu, S. Rajan, A. Mayers, and D. A. Gregory, "Optical Novelty Filter with Phase Carrier," Optics. Comm. **92**, 205-208 (1992).

18. G. Yang and A. Siahmakoun, "Time-Delay Fizeau Phase-Conjugate Interferometer," Appl. Opt. **32**, 1578-1582 (1993).

19. V. V. Shkunov and B. Y. Zel'dovich, "Optical Phase Conjugation," Sci. Am. **253**(6), 54-59 (1985).

20. D. M. Bloom, P. F. Liao, and N. P. Economou, "Observation of Amplified Reflection by degenerate Four-Wave-Mixing in Atomic Sodium Vapor," Opt. Lett. **2**, 58-60 (1978).

21. S. H. Lee, Ed., *Optical Information Processing, Fundamentals* (Springer-Verlag, Berlin, 1981), pp. 150-151.

22. P. F. Liao and D. M. Bloom, "Continuous-Wave Backward-Wave Generation by Degenerate Four-Wave Mixing in Ruby," Opt. Lett. **3**, 4-6 (1978).

23. T. W. Mossberg, R. Kachru, S. R. Hartmann, and A. M. Flusberg, "Echoes in Gaseous Media: A Generalized Theory of Rephasing Phenomena," Phys. Rev. A **20**, 1976-1996 (1979).

24. X. A. Shen, A-D. Nguyen, J. W. Perry, D. L. Huestis, and R. Kachru, "Time-Domain Holographic Digital Memory," Science **278**, 96-100 (1997).

25. T. W. Mossberg, "Time-Domain Frequency-Selective Optical Data Storage," Opt. Lett. **7**, 77-79 (1982).

26. H. M. Smith, *Principles of Holography* (Wiley, New York, 1975), pp. 227-231.

27. H. J. Caufield, *Handbook of Optical Holography* (Academic, San Diego, CA, 1979), pp. 491-493.

28. A. A. Kaplyanskii and R. M. Macfarlane, Eds, *Spectroscopy of Solids Containing Rare Earth Ions* (Elsevier Science, Amsterdam, 1987), pp. 78-80.

29. R. Yano, M. Mitsunaga, and N. Uesugi, "Ultralong Optical Dephasing Time in Eu^{3+}:Y_2SiO_5," Opt. Lett. **16,** 1884-1886 (1991).

30. A. Yariv, *Quantum Electronics* (Wiley, New York, 1975), pp. 334-335.

31. R. W. Equall, Y. Sun, R. L. Cone, and R. M. Macfarlane, "Ultraslow Optical Dephasing in Eu^{3+}:Y_2SiO_5," Phys. Rev. Lett. **72,** 2179-2182 (1994).

32. R. W. Equall, R. L. Cone, and R. M. Macfarlane, "Homogeneous Broadening and Hyperfine Structure of Optical Transitions in Pr^{3+}:Y_2SiO_5," Phys. Rev. B **52**, 3963-3969 (1995).

33. G. Birkhoff and E. H. Zarantonello, *Jets, Wakes, and Cavities* (Academic Press, New York, 1957), pp. 294-295.

APPENDIX A

ANALYSIS FOR NOVELTY AND MONOTONY CHANNEL OUTPUT

If the beamsplitter in the interferometer is exactly 50/50, the ratio of novelty and monotony $I(y)/I(x)$ is proportional to $(1 - \cos\delta)/(1 + \cos\delta)$. In reality, the beamsplitter is not exactly 50/50 and more careful analysis is necessary as follows.

The amplitudes of the echoes on the two arms are E and E', respectively (see Figure 4). The beamsplitter in the interferometer has reflection and transmission coefficients of r and t in amplitude, respectively. r^2 and t^2 are close to 50%. The amplitude of the echoes that finally fall on the two detectors is $E_y = (Er - E't)a$ for novelty output (channel y) and $E_x = (Et + E'r)b$ for monotony output (channel x), where a and b are constants that include all loss factors. We assume the intensities of the two echoes are equal at the novelty output. In other words, $I(y,e) = I(y,e') = I(e)$ when either arm is blocked. Under this condition, the two echoes at the novelty output differ only in phase, i.e., $E't/Er = e^{i\delta}$.

Let $f = (r/t)^2$ and $q = (b/a)^2$. Then the novelty output is

$$I(y) = E_y E_y^* = 2(1 - \cos\delta)I(e)$$

and the monotony output intensity is

$$I(x) = E_x E_x^* = 2(p + q\cos\delta)I(e)$$

where $p = q(f^2 + 1)/2f$. Finally, $I(y)/I(x) = (1 - \cos\delta)/(p + q\cos\delta)$.

To find p and q, we need to measure the ratio between the two channels when one of the arms is blocked. In the novelty output, $I(y,e) = I(y,e') = I(e)$. In the monotony output, $I(x,e) = I(e)(q/f)$ when E' is blocked, and $I(x,e') = I(e)(qf)$ when E is blocked.

Thus, if we measure the ratio $s(e) = I(y,e)/I(x,e)$ when E' is blocked and $s(e') = I(y,e')/I(x,e')$ when E is blocked, then $f^2 = s(e)/s(e')$ and $(1/q)^2 = s(e)s(e')$. From this, we find p and q.

APPENDIX B

DERIVATION OF AVERAGE OF NOVELTY OUTPUT WHEN SAMPLING PERIODIC OSCILLATION

The novelty filter output is $\sim[1 - \cos\delta]$, where δ is the change of optical path length over the response time. When $\delta < 1$, the filter's output is $\sim \delta^2$.

For a sinusoidally oscillating optical path length,

$$\delta \sim \sin[\omega(t_i + T)] - \sin(\omega t_i)$$

where ω is the oscillation frequency, t_i is the time when the laser samples the medium, and T is the novelty filter's response time. Thus

$$\delta^2 \sim \sin^2[\omega(t_i + T)] + \sin^2(\omega t_i) - 2\sin[\omega(t_i + T)]\sin(\omega t_i).$$

Because the laser is not synchronous with the oscillation, t_i is a random sampling time. If we take the average of many laser shots,

$$\langle\delta^2\rangle \sim 1/2 + 1/2 + \langle\cos[\omega(2t_i + T)] - \cos(\omega T)\rangle = 1 - \cos(\omega T).$$